Potential Protection Against Type 2 Diabetes in Obesity Through Lower CD36 Expression and Improved Exocytosis in β-Cells

Mototsugu Nagao,[1,2] Jonathan L.S. Esguerra,[1] Akira Asai,[1,2,3] Jones K. Ofori,[1] Anna Edlund,[1] Anna Wendt,[1] Hitoshi Sugihara,[2] Claes B. Wollheim,[4] Shinichi Oikawa,[2] and Lena Eliasson[1]

Diabetes 2020;69:1193–1205 | https://doi.org/10.2337/db19-0944

Obesity is a risk factor for type 2 diabetes (T2D); however, not all obese individuals develop the disease. In this study, we aimed to investigate the cause of differential insulin secretion capacity of pancreatic islets from donors with T2D and non-T2D (ND), especially obese donors (BMI ≥30 kg/m^2). Islets from obese donors with T2D had reduced insulin secretion, decreased β-cell exocytosis, and higher expression of fatty acid translocase CD36. We tested the hypothesis that CD36 is a key molecule in the reduced insulin secretion capacity. Indeed, CD36 overexpression led to decreased insulin secretion, impaired exocytosis, and reduced granule docking. This was accompanied by reduced expression of the exocytotic proteins SNAP25, STXBP1, and VAMP2, likely because CD36 induced downregulation of the insulin receptor substrate (IRS) proteins, suppressed the insulin-signaling phosphatidylinositol 3-kinase/AKT pathway, and increased nuclear localization of the transcription factor FoxO1. CD36 antibody treatment of the human β-cell line EndoC-βH1 increased IRS1 and exocytotic protein levels, improved granule docking, and enhanced insulin secretion. Our results demonstrate that β-cells from obese donors with T2D have dysfunctional exocytosis likely due to an abnormal lipid handling represented by differential CD36 expression. Hence, CD36 could be a key molecule to limit β-cell function in T2D associated with obesity.

Hyperglycemia caused by insufficient insulin action characterizes type 2 diabetes (T2D). Insulin resistance and defective insulin secretion are the two major pathogenic factors of the disease, and both are strongly associated with lifestyle and genetic components (1,2). Obesity is one of the strong risk factors for the development of T2D. In obesity, lipid accumulation is common not only in adipose tissue but also in ectopic tissues such as the liver and skeletal muscle. The intracellular lipid accumulation in ectopic tissues leads to impaired insulin signaling and promotes systemic insulin resistance (3). However, not all obese individuals develop T2D because pancreatic β-cells can adjust, to a certain extent, for an increasing demand of insulin. Pancreatic β-cell dysfunction is central in the failure to adjust for the increased insulin resistance. Indeed, reduced first-phase insulin response can, at least in some individuals, be observed already before the development of T2D (4). These findings suggest that those who cannot adapt to the extra demand by increased insulin secretion are prone to T2D.

Like insulin target tissues, the insulin-producing β-cells have been shown to be damaged by excessive lipid accumulation, a concept known as β-cell lipotoxicity (5). In this condition, accumulated lipids, specifically triacylglycerol, cause cellular stress, dysfunction, and death of the β-cell. In fact, increased accumulation of lipid droplets is observed with increased BMI in human β-cells (6). A number of in vitro studies have identified mechanisms involved in impaired insulin secretion by chronic fatty acid (FA) elevation (7,8), including those affecting exocytosis (9).

[1]Department of Clinical Sciences, Malmö, Islet Cell Exocytosis, Lund University Diabetes Centre, Lund University, Clinical Research Centre, Malmö, Sweden
[2]Department of Endocrinology, Diabetes and Metabolism, Graduate School of Medicine, Nippon Medical School, Tokyo, Japan
[3]Food and Health Science Research Unit, Graduate School of Agricultural Science, Tohoku University, Sendai, Japan
[4]Department of Cell Physiology and Metabolism, Faculty of Medicine, University of Geneva, Geneva, Switzerland

Corresponding authors: Lena Eliasson, lena.eliasson@med.lu.se, and Mototsugu Nagao, s8067@nms.ac.jp

Received 19 September 2019 and accepted 9 March 2020

This article contains supplementary material online: https://doi.org/10.2337/db20-4567/suppl.11965530.

Moreover, insulin signaling in β-cells is essential not only for growth but also for proper regulation of the cellular function (10–12). Hence, together these findings indicate that insulin resistance and defective insulin secretion are likely to share common etiologies in terms of lipid accumulation. Both endogenous FA synthesis and FA uptake are considered causally important for increased lipid accumulation in β-cells (13,14).

We show in this study that, among human donors with obesity, insulin secretion capacity of pancreatic islets and β-cell exocytosis were significantly lower in donors with T2D than in non-T2D (ND). We compared expression levels of the FA transporters in their islets to address the role of facilitated FA uptake for the defective insulin secretion. We further explored in detail the signaling pathway involved in CD36-modulated insulin secretion in β-cells using INS-1 cells carrying a Tet-on system for CD36 overexpression. Finally, we tested the therapeutic potential of a CD36-neutralizing antibody to improve β-cell function in human EndoC-βH1 cells.

RESEARCH DESIGN AND METHODS

Cell Line and Culture

INS-1 cells carrying the Tet-on system for CD36 overexpression (15) were cultured with RPMI 1640 medium containing 11.1 mmol/L glucose, 10% FBS, 100 IU/mL penicillin, 100 μg/mL streptomycin, 50 mg/mL neomycin, 50 mg/mL hygromycin, 10 mmol/L HEPES, 1 mmol/L sodium pyruvate, and 50 μmol/L β-mercaptoethanol at 37°C in a humidified atmosphere with 5% CO_2. To induce CD36 expression, cells were seeded in 24- or 48-well plates and cultured with or without 500 ng/mL doxycycline (Sigma-Aldrich, St. Louis, MO) for 72 h.

EndoC-βH1 cells (16) were cultured in Matrigel/fibronectin-coated (100 μg/mL and 2 μg/mL, respectively) (Sigma-Aldrich) vessels with DMEM containing 5.6 mmol/L glucose, 2% BSA, 10 mmol/L nicotinamide, 50 μmol/L β-mercaptoethanol, 5.5 μg/mL transferrin, 6.7 ng/mL sodium selenite, 100 IU/mL penicillin, and 100 μg/mL streptomycin at 37°C in a humidified atmosphere with 5% CO_2. Cells were seeded in Matrigel/fibronectin-coated 48-well plates and cultured for 72 h with 2 μg/mL of a CD36-blocking antibody (FA6.125, catalog number 60084; STEMCELL Technologies, Vancouver, British Columbia, Canada) or an isotype control (MOPC-21, catalog number ab18443; Abcam, Cambridge, U.K.).

Human Pancreatic Islets

Human pancreatic islets were obtained from cadaver donors of European ancestry by the Nordic Network for Clinical Islet Transplantation. The islets were processed as previously described (17) and handpicked under stereomicroscope before use. To dissociate into single cells, the islets were incubated with 3 mmol/L EGTA in Hanks' balanced salt solution containing 0.25% BSA for 15 min at 37°C followed by gentle pipetting. Donor characteristics for each experiment are shown in Supplementary Table 1. All procedures using human islets were approved by the ethical committees in Uppsala and Malmö/Lund, Sweden.

Human Islet RNA-Sequencing Data Analysis

Islet RNA-sequencing (RNA-seq) data were retrieved from the Gene Expression Omnibus with accession numbers GSE50398 and GSE108072 from the studies of Fadista et al. (18) and Gandasi et al. (19), respectively. The expression values are expressed as log2 counts per million after normalization and transformation using voom. Expression levels of selected genes were retrieved from 68 normal-body-weight (BMI <25 kg/m^2) and 31 obese (BMI ≥ 30 kg/m^2) donors.

Insulin Secretion Assay

For CD36 INS-1 cells, after being washed twice with 1 mL prewarmed secretion assay buffer (SAB) (1.16 mmol/L $MgSO_4$, 4.7 mmol/L KCl, 1.2 mmol/L KH_2PO_4, 114 mmol/L NaCl, 2.5 mmol/L $CaCl_2$, 25.5 mmol/L $NaHCO_3$, 20 mmol/L HEPES, and 0.2% BSA, pH 7.2) with 2.8 mmol/L glucose, cells were preincubated in 0.5 mL SAB with 2.8 mmol/L glucose for 1 h. The cells were then stimulated for 1 h in 0.25 mL SAB with 2.8 mmol/L glucose or 16.7 mmol/L glucose or for 15 min in 0.25 mL SAB with 2.8 mmol/L glucose and 50 mmol/L KCl at 37°C. Secreted insulin levels were measured using Rat Insulin ELISA (Mercodia, Uppsala, Sweden), and the values were normalized to the protein content. Protein was extracted with 100 μL RIPA buffer (0.1% SDS, 150 nmol/L NaCl, 1% Triton X-100, and 50 mmol/L Tris-HCl, pH 8.0), and the content was analyzed using a BCA Protein Assay Kit (Thermo Fisher Scientific).

For EndoC-βH1 cells, culture medium was changed to a medium containing 2.8 mmol/L glucose and further incubated for 18 h before the secretion assay. After two washes with 1 mL SAB containing 1 mmol/L glucose, cells were preincubated in 0.5 mL SAB with 1 mmol/L glucose for 2 h. The cells were then stimulated for 15 min with 0.25 mL SAB with 1 mmol/L glucose or 20 mmol/L glucose at 37°C. Secreted insulin levels were measured using Human Insulin ELISA (Mercodia), and the values were normalized to the protein content. Protein content was measured as above.

For human islets, glucose-stimulated insulin secretion was examined using a dynamic glucose perifusion system to calculate the stimulation index as a quality control (20). To evaluate membrane depolarization-induced insulin secretion, batches of 12 islets were preincubated for 30 min in Krebs-Ringer bicarbonate buffer, pH 7.4, supplemented with 20 mmol/L HEPES, 0.1% BSA, and 1 mmol/L glucose and then stimulated for 1 h in Krebs-Ringer bicarbonate buffer with 70 mmol/L KCl and 1 mmol/L glucose.

Insulin-Stimulation Assay

Insulin-stimulation assay was performed on the confluent cells after 72 h of seeding. After washing with prewarmed PBS twice, the cells were preconditioned with the FBS-free culture medium containing 1 mmol/L glucose for 6 h to

diminish an autocrine effect of insulin on the signaling pathway. The cells were then stimulated for 10 min in the conditioning medium without (0) or with 1 or 10 nmol/L human insulin (Actrapid Penfill; Novo Nordisk, Bagsværd, Denmark). After discarding the medium, the cells were frozen immediately in liquid nitrogen and lysed with one-time loading buffer, followed by sonication. The cell lysates were stored at −80°C until Western blot analysis.

Subcellular Fractionation

Subcellular fractionation of CD36 INS-1 cells was performed using a Subcellular Protein Fractionation Kit for Cultured Cells (Thermo Fisher Scientific). Purity of each fraction was verified by Western blot analysis.

Western Blot Analysis

Protein samples (7.5–10 μg protein/sample) were applied to SDS-PAGE using 4–15% TGX Stain-Free gels (Bio-Rad Laboratories, Hercules, CA). The gels were then activated with ultraviolet light for 1 min to visualize total protein on the blotted low-fluorescence polyvinylidene difluoride membrane using the Stain-Free technology (Bio-Rad Laboratories). Blotting was performed using a Trans-Blot Turbo Transfer System (Bio-Rad Laboratories). The membrane blocking and incubation with primary antibodies were performed with 5% skim milk in Tris-buffered saline with Tween, except for phosphorylated proteins with 3% BSA in Tris-buffered saline with Tween. Primary antibodies and their dilutors are provided in Supplementary Table 2. Incubation with the primary antibodies was performed overnight at 4°C. Horseradish peroxidase–conjugated anti-rabbit (catalog number 170–6515; 1:2,000; Bio-Rad Laboratories), anti-mouse (catalog number P0447, 1:2,000; Agilent Technologies, Santa Clara, CA), and anti-goat (catalog number ab6741; 1:1,000; Abcam) Igs were used as secondary antibodies. Incubation with the secondary antibodies was performed for 1 h at room temperature. Clarity Western ECL Substrate (Abcam) or SuperSignal West Femto Maximum Sensitivity Substrate (Thermo Fisher Scientific) was used for visualization of proteins with a ChemiDoc XRS+ System (Bio-Rad Laboratories). The signal intensity of each protein band was measured using Image Lab Software (version 5.2.1; Bio-Rad Laboratories) and normalized to that of the total protein bands in the lane, except for the phosphorylated protein band, which was normalized to the corresponding total protein band.

Electrophysiology

Whole-cell patch-clamp experiments were conducted on single human β-cells (cell capacitance >9 pF) or CD36 INS-1 cells as described previously (21). The recordings were performed using an EPC 10 patch-clamp amplifier with Patchmaster software (ver. 2–73; HEKA Elektronik, Lambrecht, Germany). Exocytosis was evoked by a train of 10 500-ms depolarizations from −70 to 0 mV applied at 1 Hz. Voltage-dependent currents were investigated using a current-voltage protocol in which the membrane was depolarized from −70 mV to voltages between −40 and +40 mV during 50 ms. The sustained current (I), measured during the latter 20 ms of the depolarizations, was considered as Ca^{2+} current.

Immunocytochemistry

Dissociated islet cells or CD36 INS-1 cells were fixed and stained as described elsewhere (22). Primary antibodies for CD36 (JC63.1, catalog number ab23680, 1:200; Abcam), insulin (catalog number 03–16049; 1:400; American Research Products, Inc., Waltham, MA), Na^+K^+ ATPase (catalog number ab76020; 1:200; Abcam), and FoxO1 (catalog number 2880; 1:200; Cell Signaling Technology) diluted in blocking buffer were treated for 2 h. After washing twice with PBS, the cells were exposed to fluorescent-labeled corresponding secondary antibodies (1:400) for 1 h, followed by postfixation with 3% paraformaldehyde in PBS. Immunofluorescence was observed with a confocal microscope (Meta 510 or LSM 880; Carl Zeiss, Oberkochen, Germany). Nuclear localization of FoxO1 was evaluated by the nuclear fluorescence intensity normalized to the whole-cell intensity. The nuclear region was defined by DAPI staining. The fluorescence intensity was analyzed with ZEN software (Carl Zeiss).

Flow Cytometry

Dissociated islet cells were stained with allophycocyanin (APC)–conjugated anti-CD36 (catalog number 562744; BD Biosciences) for 30 min in PBS with 0.5% BSA and 0.05% sodium azide. The cells were then fixed with 3.7% paraformaldehyde in PBS for 20 min and further stained intracellularly with Alexa Fluor 488–conjugated anti-insulin (catalog number IC1417A; R&D Systems) and phycoerythrin-conjugated anti-glucagon (catalog number 565860; BD Biosciences) for 30 min in 0.1% saponin in PBS with 0.5% BSA and 0.05% sodium azide. After the cells were postfixed with 1% paraformaldehyde, flow cytometric analysis was performed using a CytoFLEX flow cytometer (Beckman Coulter, Brea, CA) with CytExpert software (version 2.0; Beckman Coulter).

RNA Extraction, RT-PCR, and Quantitative PCR

Total RNA from CD36 INS-1 cells was extracted, and cDNA was generated as described (23). Quantitative PCR was performed in 384-well plates on a ViiA 7 Real-Time PCR System (Thermo Fisher Scientific) using TaqMan Gene Expression Assays with Universal PCR Master Mix (Thermo Fisher Scientific). Rat *Hprt1* (assay identification number: Rn01527840_m1; Applied Biosystems) and *Ppia* (assay identification number: Rn00690933_m1) were used for normalization. Relative expression was calculated using the ΔΔ threshold cycle method.

Transmission Electron Microscopy

CD36 INS-1 and EndoC-βH1 cells were prepared for electron microscopy, examined, and analyzed as previously described (24). Granules (large dense-core vesicles) were defined as docked when the center of the granule was located within 100 nm and 120 nm from the plasma membrane for CD36 INS-1 and EndoC-βH1, respectively. The distance

between the center of the granule and the plasma membrane was calculated using an in-house software programmed in MATLAB 7 (The MathWorks, Inc., Natick, MA).

Statistical Analysis

Data are presented as mean ± SE. The differences between two groups were analyzed by Student *t* test with two-tailed analysis. All statistical analyses were performed using Prism (version 7.0; GraphPad Software, San Diego, CA).

Data and Resource Availability

The data sets generated and/or analyzed during the current study are available from the corresponding authors on reasonable request. The CD36-overexpressing INS-1 cell line may be available from Prof. Anneli Björklund (Karolinska Institute, Stockholm, Sweden) upon reasonable request and with permission of the founder, C.B.W.

RESULTS

Reduced Islet Insulin Secretion and β-Cell Exocytosis in Donors With T2D and Obesity

We investigated insulin secretion capacity of pancreatic islets in donors with T2D and ND with normal body weight (BMI <25 kg/m^2) or obesity (BMI ≥30 kg/m^2). Islets of donors with T2D in both BMI categories showed reduced glucose-stimulated insulin secretion as compared with those of ND (Fig. 1*A* and *B*). Basal insulin secretion was decreased only in islets of donors with T2D with normal body weight (Fig. 1*A*). Accordingly, decreased insulin-stimulation index in islets of T2D was confirmed only among donors with obesity (Supplementary Fig. 1). Static incubation with K^+ also revealed significantly decreased insulin secretion in islets of T2D as compared with ND among donors with obesity, albeit a similar basal insulin secretion (Fig. 1*C* and *D*), suggesting defects downstream of the ATP-dependent K^+ channel. Indeed, capacitance recordings on single β-cells evoked by a train of 10 500-ms depolarizations from −70 to 0 mV demonstrated reduced Ca^{2+}-dependent exocytosis in β-cells of obese donors with T2D as compared with those of obese donors with ND (Fig. 1*E*).

Differential Islet CD36 Expression Between Donors With T2D and ND With Obesity

We next compared gene expression levels of FA transporters (CD36 and SLC27 family) in RNA-seq data of human pancreatic islets deposited in the Gene Expression Omnibus

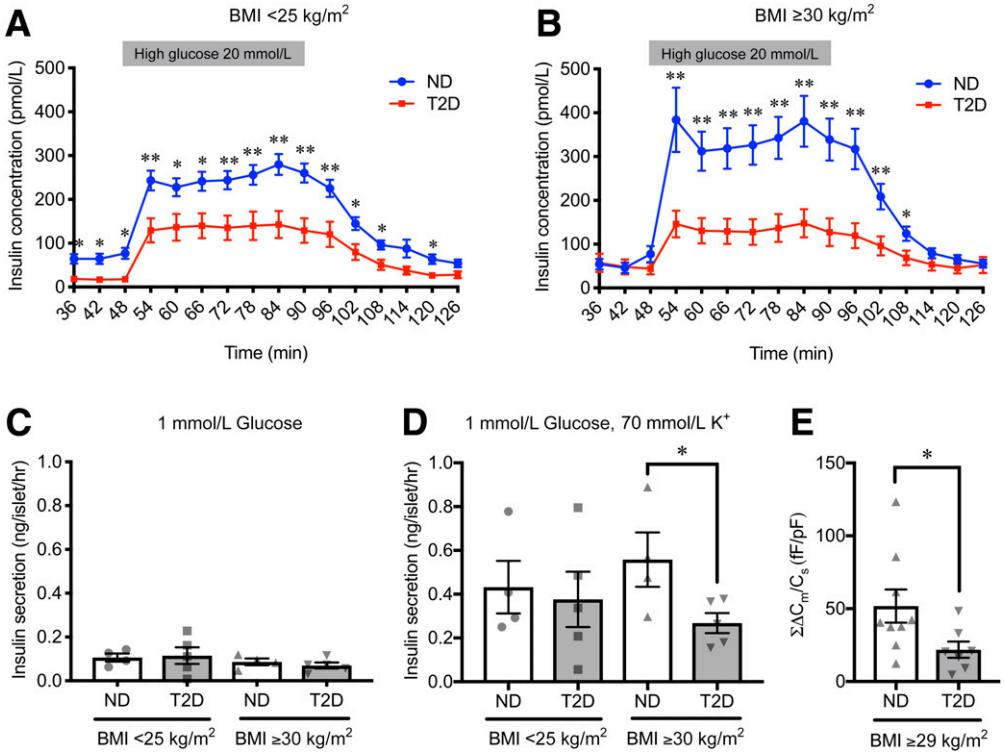

Figure 1—Characteristics of pancreatic islets from donors with ND and T2D with normal body weight and with obesity. *A* and *B*: Insulin-release curves in response to dynamic glucose perfusion. Islets from donors with ND (blue) and T2D (red) with normal body weight (*A*) (ND, $n = 38$ donors; T2D, $n = 14$ donors) and with obesity (*B*) (ND, $n = 11$ donors; T2D, $n = 12$ donors) were subjected to dynamic perifusion at low (1.67 mmol/L) and high glucose (20 mmol/L) solutions. High glucose was added from 48 to 90 min, whereas other fractions were exposed to low glucose (1.67 mmol/L). Insulin secretion in static incubation at 1 mmol/L glucose (*C*) and 1 mmol/L glucose with 70 mmol/L K^+ for 1 h (*D*) in islets from donors with ND and T2D with normal body weight (ND, $n = 4$ donors; T2D, $n = 5$ donors) and obesity (ND, $n = 4$ donors; T2D, $n = 5$ donors). *E*: Total cell capacitance changes ($\Sigma\Delta C_m$), reflecting exocytosis, evoked by a train of 10 500-ms depolarizations from −70 to 0 mV in β-cells from donors with ND ($n = 9$ cells from 5 donors) and T2D ($n = 7$ cells from 3 donors) with high BMI (BMI ≥29 kg/m^2). All data were normalized to the cell size by the measured whole-cell capacitance (C_s). The *P* values were determined by Student two-tailed *t* test (unpaired). *$P < 0.05$; **$P < 0.01$. fF, femtofarad; hr, hour; pF, picofarad.

(GSE50398 and GSE108072) to investigate the role of facilitated FA uptake for defective insulin secretion observed in the islets of donors with T2D and obesity (Fig. 2*A* and Supplementary Fig. 2). Differences were observed in *CD36* and *SLC27A3* expression between ND (HbA_{1c} <6% [42 mmol/mol]) and impaired glucose tolerance (IGT)/T2D (HbA_{1c} ≥6.0% [42 mmol/mol] or those previously diagnosed with T2D) among donors with obesity. Within the group of FA transporters, *CD36* was the most abundantly expressed in human islets. Interestingly, CD36 expression was lower in islets from the obese donors with ND as compared with the other three groups. We further validated the RNA-seq findings by Western blot analysis of human islets. CD36 protein expression in islets from obese donors with T2D was 70% higher than that in islets from obese donors with ND (Fig. 2*B* and *C*). We also confirmed CD36 protein expression in human β-cells using confocal microscopy (Fig. 2*D*). A semiquantitative analysis of the confocal images suggests that CD36 is expressed equally in the cytosol and on the plasma membrane (Supplementary Fig. 3). A flow cytometry analysis further revealed that CD36 is localized on the outer surface of the plasma membrane (Fig. 2*E* and *F*).

CD36 Impairs Exocytosis by Inhibiting Granule Docking in β-Cells

To evaluate the mechanisms by which CD36 effects insulin secretion, we investigated insulin secretion in INS-1 cells carrying a Tet-on system for CD36 overexpression (25). Doxycycline induced CD36 expression dose dependently (Supplementary Fig. 4*A*), and the induced CD36 protein was located on the plasma membrane (Fig. 3*A*). We observed

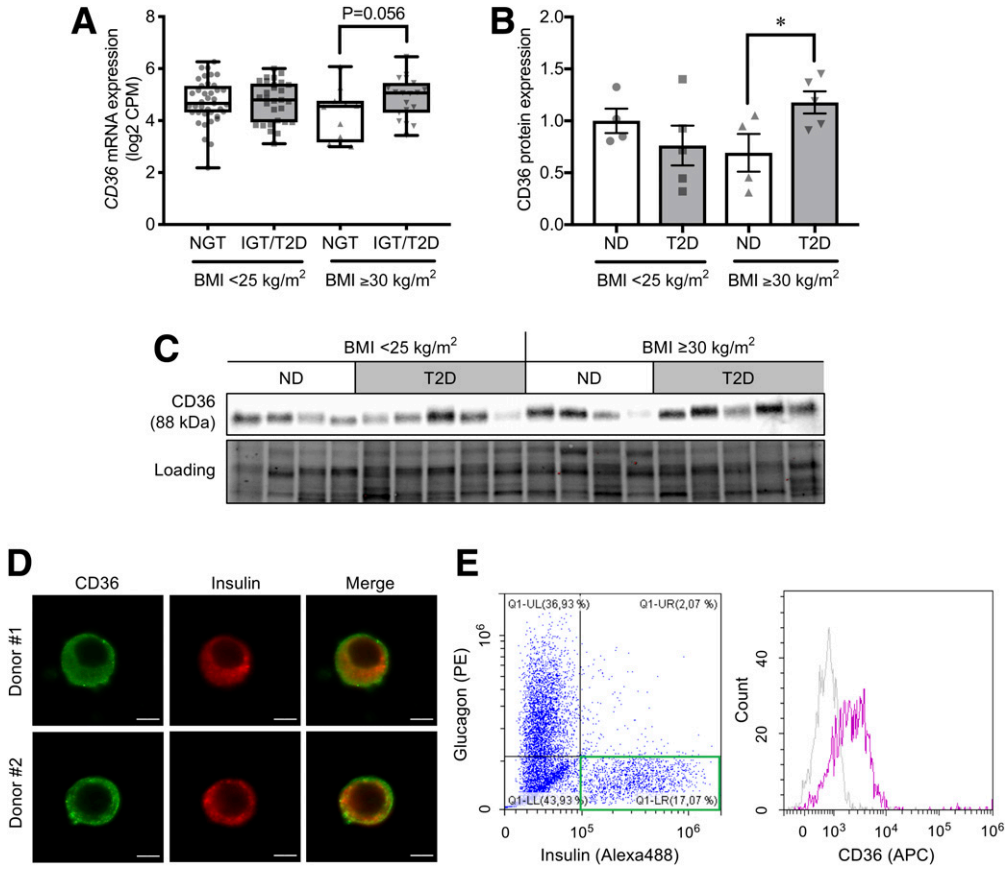

Figure 2— Expression of CD36 in human pancreatic islets. *A*: *CD36* mRNA levels in islets from donors with ND (HbA_{1c} <6.0%) and IGT/T2D (HbA_{1c} ≥6.0%) with normal body weight (BMI <25 kg/m^2; ND, n = 39 donors; IGT/T2D, n = 29 donors) and with obesity (BMI ≥30 kg/m^2; ND, n = 12 donors; IGT/T2D, n = 19 donors). The box extends from the 25th to 75th percentiles. The line in the middle of the box is plotted at the median. The whiskers go down to the smallest value and up to the largest. CD36 protein levels (*B*) and the Western blotting bands (*C*) in islets from donors with ND and T2D with normal body weight (ND, n = 4 donors; T2D, n = 5 donors) and with obesity (ND, n = 4 donors; T2D, n = 5 donors). The total protein images obtained using the Stain-Free technology are shown as a loading control (Loading). *D*: Immunocytochemical images of CD36 (green) expression in insulin-positive (red) islet cells from two different human donors. Scale bars, 5 μm. *E* and *F*: Flow cytometric analysis of human islet cells. Pancreatic islets were dissociated into a single cell suspension and extracellularly stained for CD36 (APC) followed by intracellular staining for insulin (Alexa 488) and glucagon (phycoerythrin [PE]). Insulin-positive glucagon-negative cells within a green square were defined as β-cells (*E*), and the β-cell surface CD36 (APC) expression was analyzed with anti-CD36 antibody (purple) and isotype control (gray) (*F*). The *P* values were determined by Student two-tailed *t* test (unpaired). *P < 0.05. CPM, counts per million.

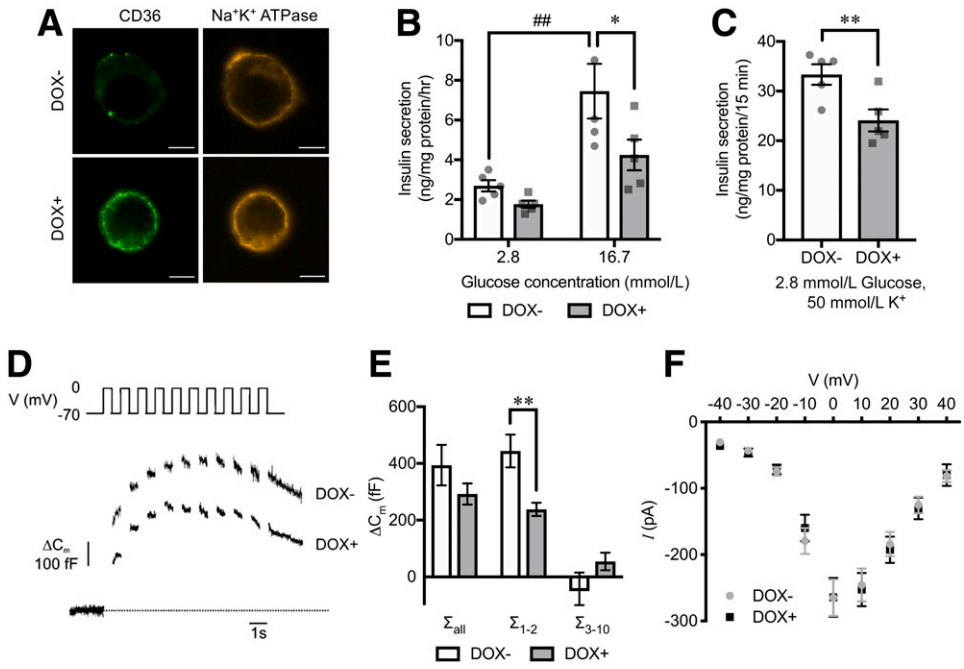

Figure 3— Insulin secretion and exocytosis in CD36-overexpressing INS-1 cells. *A*: Immunocytochemical images of CD36 (green) in INS-1 cells without (DOX−) or with doxycycline-induced CD36 overexpression (DOX+). Na^+-K^+ ATPase (orange) was stained for a plasma membrane marker. Scale bars, 5 μm. Insulin secretion at 2.8 mmol/L or 16.7 mmol/L glucose for 1 h (*B*) and at 2.8 mmol/L glucose with 50 mmol/L K^+ for 15 min (*C*). $N = 5$ for each group. Representative cell capacitance changes evoked by a train of 10 500-ms depolarizations from −70 to 0 mV (*D*) and the sum of capacitance increase (ΔC_m) in response to the depolarization pulses of the train (*E*). $N = 13$ to 14 cells for each group. *F*: Inward Ca^{2+} currents evoked by depolarizations. Current (I)–voltage (V) relationship for the peak Ca^{2+} currents. $N = 15$ to 16 cells for each group. The *P* values were determined by repeated-measures one-way ANOVA followed by Tukey honest significant difference (*B*) and Student two-tailed *t* test (paired for *C* and unpaired for *E*). $^*P < 0.05$, $^{**}P < 0.01$ vs. DOX− under the same condition; $\#\#P <$ 0.01 vs. 2.8 mmol/L glucose for each group (DOX− or DOX+). fF, femtofarad; hr, hour; pA, picoampere.

reduced glucose-stimulated insulin secretion (~40%) in INS-1 cells at 72 h after the induction of CD36 compared with control (Fig. 3*B*). Likewise, membrane depolarization by K^+ showed reduced insulin secretion by ~30% in CD36-overexpressing cells (Fig. 3*C*). CD36 overexpression did not change cellular insulin content (Supplementary Fig. 4*B*). Capacitance measurements on single cells using the patch-clamp technique (Fig. 3*D*) revealed that exocytosis, evoked by a train of 10 depolarizations (Σ_{all}), was reduced by ~25% in CD36-overexpressing cells, which did not reach significance due to endocytosis evoked by the latter depolarizations (Fig. 3*E*). The reduction in membrane capacitance increase was more prominent (and reached significance) during the first two depolarizations (Σ_{1-2}), reflecting rapid exocytosis of docked and primed granules (Fig. 3*E*). The reduced exocytosis was not a cause of changes in the inward Ca^{2+} current (Fig. 3*F*).

We next performed transmission electron microscopy (Fig. 4*A*) to estimate the granule volume density per cell (N_v) and the surface density per cell (N_s), which are proportional to the total number of granules and the number of docked granules, respectively (24). While the total number of granules within the cells was not affected by CD36 overexpression (Fig. 4*B*), the number of granules within 100 nm from the plasma membrane, regarded as the docked granule pool, was significantly reduced (Fig. 4*C* and *D*). We found expression of exocytotic genes *Snap25* and *Vamp2* to be downregulated by CD36 overexpression (Fig. 4*E*). Moreover, the downregulation of *Stxbp1* was almost significant ($P = 0.057$). CD36 overexpression significantly reduced STXBP1 and SNAP25 protein levels (Fig. 4*F*).

CD36 Suppresses the Insulin Receptor Substrate/Phosphatidylinositol 3-Kinase/AKT Signaling Pathway

Several reports suggest that exocytotic gene and protein expression in β-cells is tightly regulated by the insulin-signaling phosphatidylinositol 3-kinase (PI3K)/AKT pathway and its downstream target transcription factors (e.g., FoxO1) (26,27). We therefore examined the insulin-signaling PI3K/AKT pathway in CD36-overexpressing cells. While there were no changes in insulin receptor β protein levels (Fig. 5*A*), downstream insulin receptor substrate (IRS) 1 and IRS2 protein levels were reduced in CD36-overexpressing cells (Fig. 5*B*). Next, we found reduced phosphorylation at Ser473 of AKT (Supplementary Fig. 4*C*), a key regulatory molecule of the insulin-signaling pathway, indicating AKT inactivation. The AKT phosphorylation stimulated by exogenous insulin was also blunted by CD36 overexpression (Fig. 5*C*). This will result in retention of the transcription factor FoxO1 in the nucleus (28,29). FoxO1 is known as a potent transcriptional repressor of several exocytotic genes, including *Snap25* (26). Indeed,

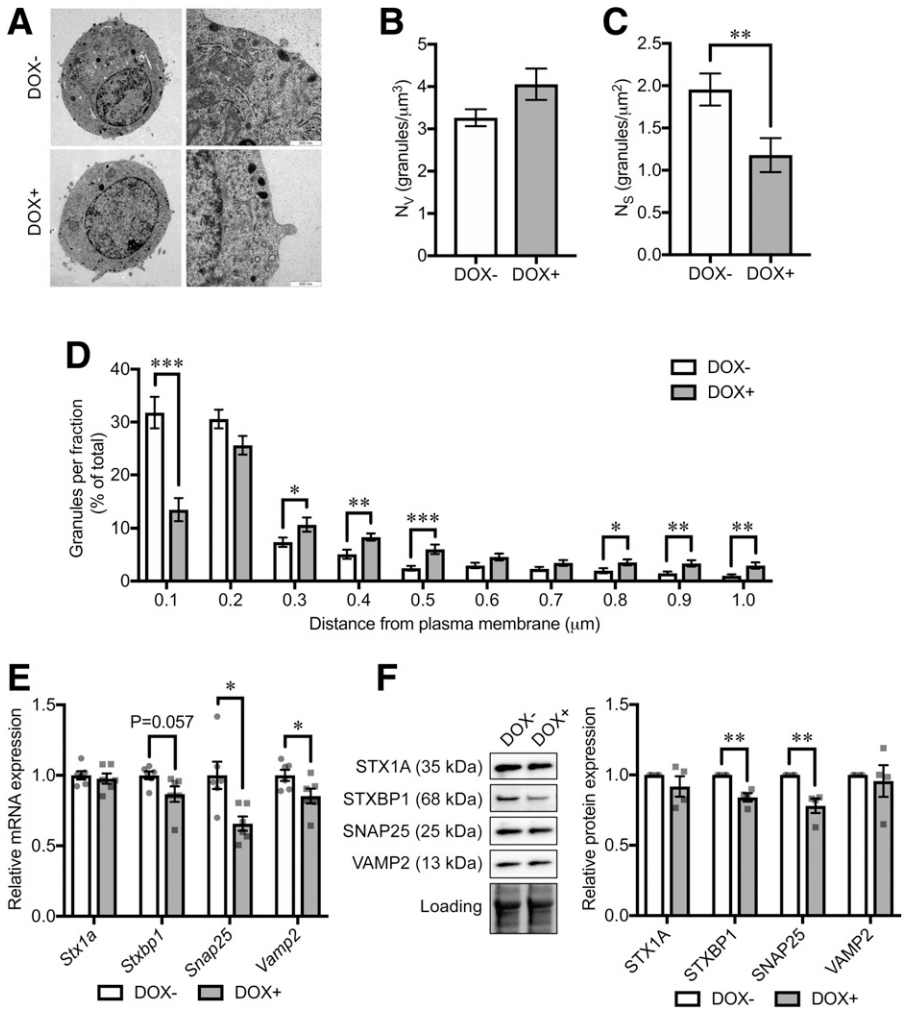

Figure 4—Insulin granule localization and exocytotic protein levels in CD36-overexpressing INS-1 cells. *A*: Electron micrographs of INS-1 cells without (DOX−) or with doxycycline-induced CD36 overexpression (DOX+). Original magnification ×6,000 (left) and ×43,000 (right). *B–D*: Granule-distribution analyses on the electron micrographs. N_v (*B*) and N_s (*C*) were measured as volume density and surface density, respectively. The granules for which the center was located within 100 nm (a half-length of the mean granule diameter) from the plasma membrane were defined as docked. Relative distribution of granules at shown distance intervals from the center of granule to the plasma membrane is shown in *D*. The distance shown in the *x*-axis is the upper border of each fraction. $N = 34–38$ cells for each group. *E*: mRNA expression levels of exocytotic genes. The expression levels were normalized to *Ppia* and *Hprt*. $N = 6$ for each group. *F:* Western blot analysis of exocytotic proteins. The total protein images obtained using the Stain-Free technology are shown as a loading control (Loading). $N = 4$ for each group. The *P* values were determined by Student two-tailed *t* test (unpaired). $^*P < 0.05$; $^{**}P < 0.01$; $^{***}P < 0.001$.

CD36 overexpression led to a significant increase in nuclear localization of FoxO1 (Fig. 5*D* and *E*).

CD36 Downregulates IRS1 Through Activation of Novel Protein Kinase C

To address the mechanism underlying the IRS downregulation in CD36-overexpressing cells, we evaluated *Irs1* and *Irs2* gene expression. In accordance with a previous report that FoxO1 in the nucleus can directly suppress *Ins2* gene expression by binding the *Irs2* promoter (30), *Irs2* gene expression was downregulated in CD36-overexpressing cells (Fig. 6*A*). However, *Irs1* transcript was not altered by CD36 overexpression in contrast to the reduced protein level (Figs. 5*B* and 6*A*), suggesting that CD36 overexpression downregulates IRS1 protein in a different way from IRS2. Because intracellular lipid accumulation has been suggested to promote IRS1 protein degradation through the activation of IκB kinase or protein kinase C (PKC) (31,32), we investigated phosphorylation of IRS1 at Ser307 and Ser612, phosphorylation targets of IκB kinase and PKC, respectively (33,34). In CD36-overexpressing cells, phosphorylation at Ser612 was increased, while no difference was observed at Ser307 as compared with the control cells (Fig. 6*B*), suggesting that CD36-induced IRS1 degradation is likely dependent on PKC activation. Among various PKC isoforms, two novel subtype PKCs (nPKCs; i.e., PKCδ and PKCε) are postulated to have negative impacts on β-cell function (35–37). We therefore evaluated membrane translocation (and activation) of PKCδ and PKCε from the cytosol to the plasma membrane. CD36 overexpression caused

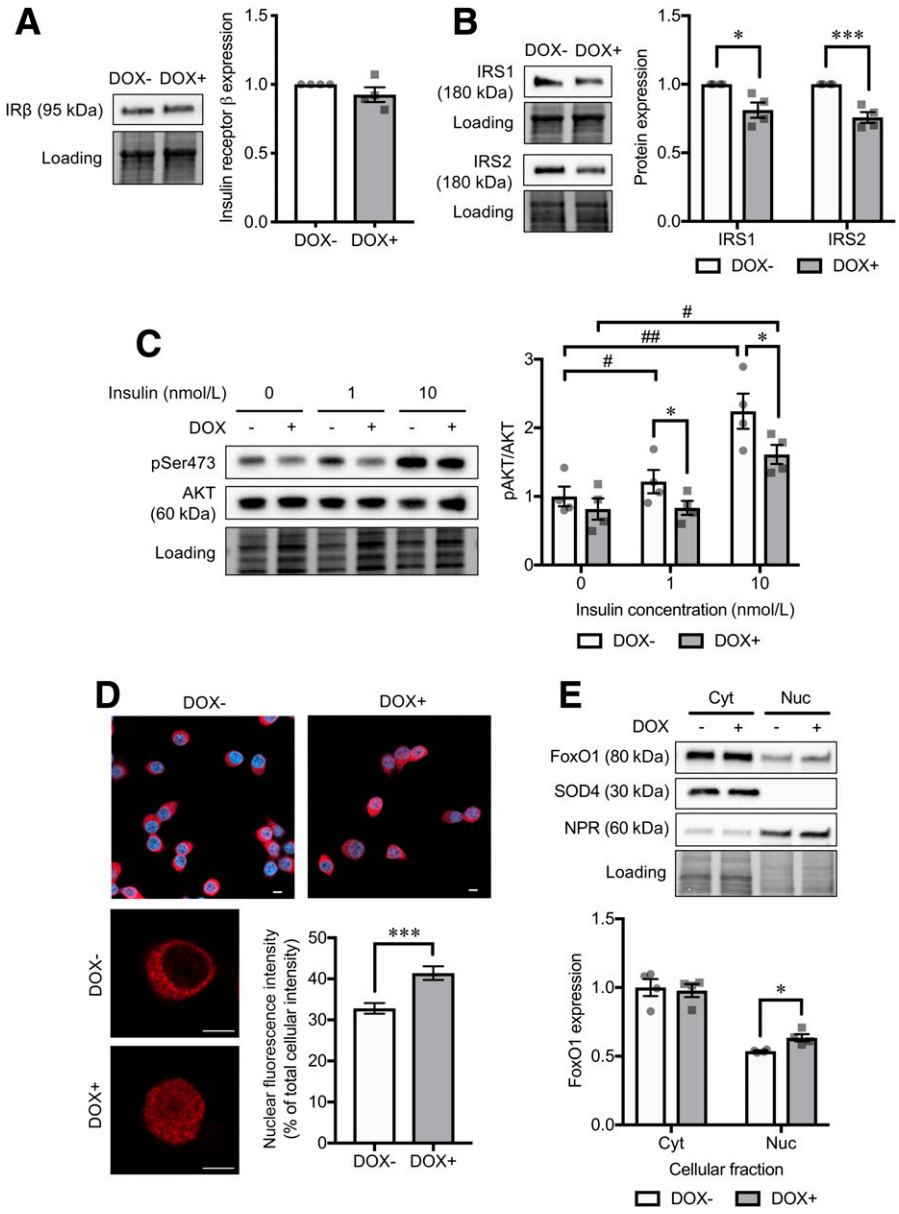

Figure 5—Analysis of insulin-signaling cascade in CD36-overexpressing INS-1 cells. Protein levels of insulin receptor β subunit (IRβ) (*A*) and IRS1 and IRS2 (*B*) in INS-1 cells without (DOX−) or with doxycycline-induced CD36 overexpression (DOX+). Normalization factor was used to adjust the target band intensity. $N = 4$ for each group. *C*: Phosphorylation levels of AKT Ser473 (pSer473) under a short-term (10-min) stimulation of insulin with various doses (1 and 10 nmol/L). Phosphorylated protein signals were normalized to the total protein levels. $N = 4$ for each group. *D*: Immunocytochemical analysis of FoxO1 (red) localization. Nuclei were stained with DAPI (blue). The bar graph shows nuclear FoxO1 fluorescence intensity normalized to the whole-cell intensity. Scale bars, 5 μm. $N = 21$ cells for each group. *E*: Western blot analysis of cytoplasmic (Cyt) and nuclear (Nuc) protein levels of FoxO1. $N = 4$ for each group. The total protein images obtained using the Stain-Free technology are shown as a loading control (Loading). The *P* values were determined by Student two-tailed *t* test (unpaired). $^{*}P < 0.05$, $^{***}P < 0.001$ vs. DOX− under the same condition; $\#P < 0.05$, $\#\#P < 0.01$ vs. cells without the stimulation of insulin (0 nmol/L) for each group (DOX− or DOX+).

a twofold increase in membrane-associated PKCε protein level (Fig. 6*C* and *D*).

Blockade of CD36 Function Improves Granule Docking and First-Phase Insulin Secretion

Finally, we investigated if blockade of CD36 function can ameliorate insulin secretion and exocytosis in β-cells. For this, we used EndoC-βH1 cells, a clonal human β-cell line (16), expressing CD36 protein (Supplementary Fig. 5). Instead of a chemical CD36 inhibitor sulfo-*N*-succinimidyl oleate, which blunts β-cell function after 72 h of coincubation (Supplementary Fig. 6), we treated the cells with a CD36-neutralizing IgG antibody (FA6.125) reported to inhibit the known functions of CD36, including FA uptake (38). Treatment with the antibody significantly increased first-phase (15-min) insulin secretion at 20 mmol/L glucose

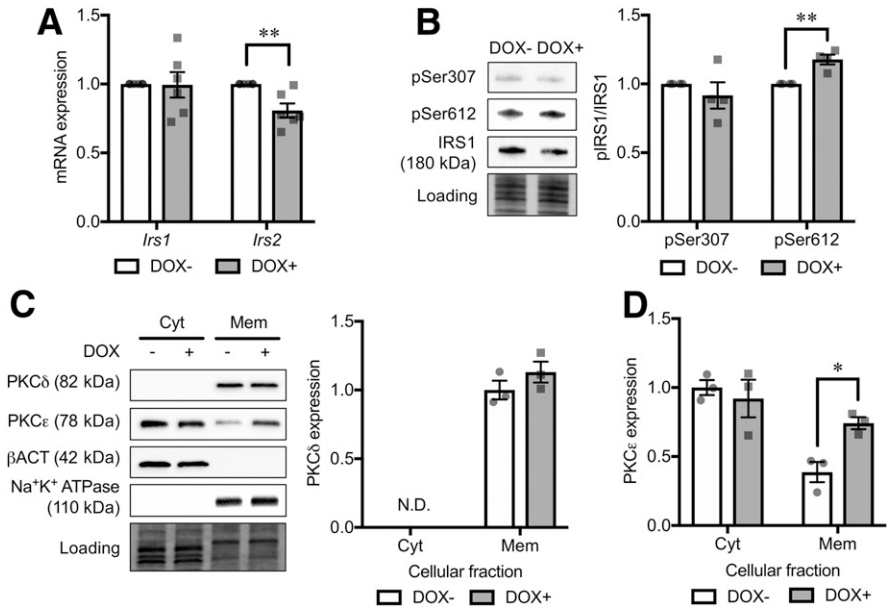

Figure 6—Analysis of background mechanism underlying IRS downregulation in CD36-overexpressing INS-1 cells. *A*: mRNA expression levels of *Irs1* and *Irs2*. The expression levels were normalized to *Ppia* and *Hprt*. $N = 6$ for each group. *B*: Phosphorylation levels of IRS1 Ser307 (pSer307) and Ser612 (pSer612). Phosphorylated protein levels were normalized to the total protein levels. $N = 4$ for each group. Western blot analysis of cytoplasmic (Cyt) and membrane (Mem) protein levels of PKCδ (*C*) and PKCε (*D*). $N = 3$ for each group. The total protein images obtained using the Stain-Free technology are shown as a loading control (Loading). DOX− and DOX+ represent INS-1 cells without and with doxycycline-induced CD36 overexpression, respectively. The *P* values were determined by Student two-tailed *t* test (unpaired). $^*P < 0.05$; $^{**}P < 0.01$. N.D., not determined.

(Fig. 7*A*). Moreover, the antibody treatment significantly increased protein levels of STX1A, SNAP25, VAMP2, and STXBP1 (Fig. 7*B*) and resulted in an increased number of docked granules (Fig. 7*C–E*). Detailed analysis revealed that the increase in N_v is mainly due to an enlargement of the granule pool closer to the plasma membrane (Fig. 7*F*), including the docked granules (N_s) and the pool regarded as the "almost" docked granules (39). In parallel, increased IRS1/2 protein levels and downstream AKT activation were observed under the blockade of CD36 function (Fig. 7*G* and *H*).

DISCUSSION

We present in this study novel human islet data and delineate the signaling pathway in CD36-dependent effects on insulin secretion. Hence, we extend previous findings of CD36 on insulin secretion (14,25). Our data show not only differential glucose-stimulated insulin secretion in islets but also a difference in β-cell exocytosis between donors with T2D and ND with obesity, suggesting that the process of exocytosis is involved in the regulation of insulin secretion capacity to compensate for insulin resistance in obesity. Indeed, CD36, which is differentially expressed in islets between donors with T2D and ND with obesity, impairs insulin secretion through the reduction of exocytotic proteins crucial for granule docking and priming in β-cells. This occurs through the downregulation of IRS1/2 and suppression of the insulin-signaling PI3K/AKT pathway and following nuclear retention of FoxO1.

One of the main functions of CD36 is a facilitated influx of long-chain FAs (LCFAs) across the plasma membrane (40). LCFA-induced β-cell dysfunction is well established (41,42), and long-term palmitate exposure of islets impairs exocytosis by dissociating Ca^{2+} channels from secretory granules (9). In contrast, CD36 overexpression inhibited exocytosis through the reduction of exocytotic protein levels and subsequent impairment of granule docking. Hence, defective exocytosis caused by CD36 is most likely a consequence of a different cellular mechanism than previously described as β-cell lipotoxicity. CD36 actually can bind not only LCFAs but also other ligands including phospholipids, ceramide, and lipoproteins (40). Considering the finding that CD36 overexpression could activate diacylglycerol (DAG)–dependent nPKCs (PKCε), FAs or other glycerolipids used for DAG synthesis are possible candidates to initiate the cellular cascade resulting in reduced exocytotic protein levels through CD36. Several studies have demonstrated the role of Fox family transcription factors on the regulation of exocytosis-related gene expression in β-cells (26,43). As FoxO1 is an established target of the insulin-signaling PI3K/AKT pathway, inhibition of the pathway actually reduces exocytotic gene and protein expression, as shown in previous studies (26,27,44). Not only FoxO1 but also other unknown transcription factors downstream of the PI3K/AKT pathway have been suggested to regulate exocytotic gene expression (e.g., constitutively active AKT [GagAkt] increased the expression of multiple exocytotic genes) (26). Furthermore,

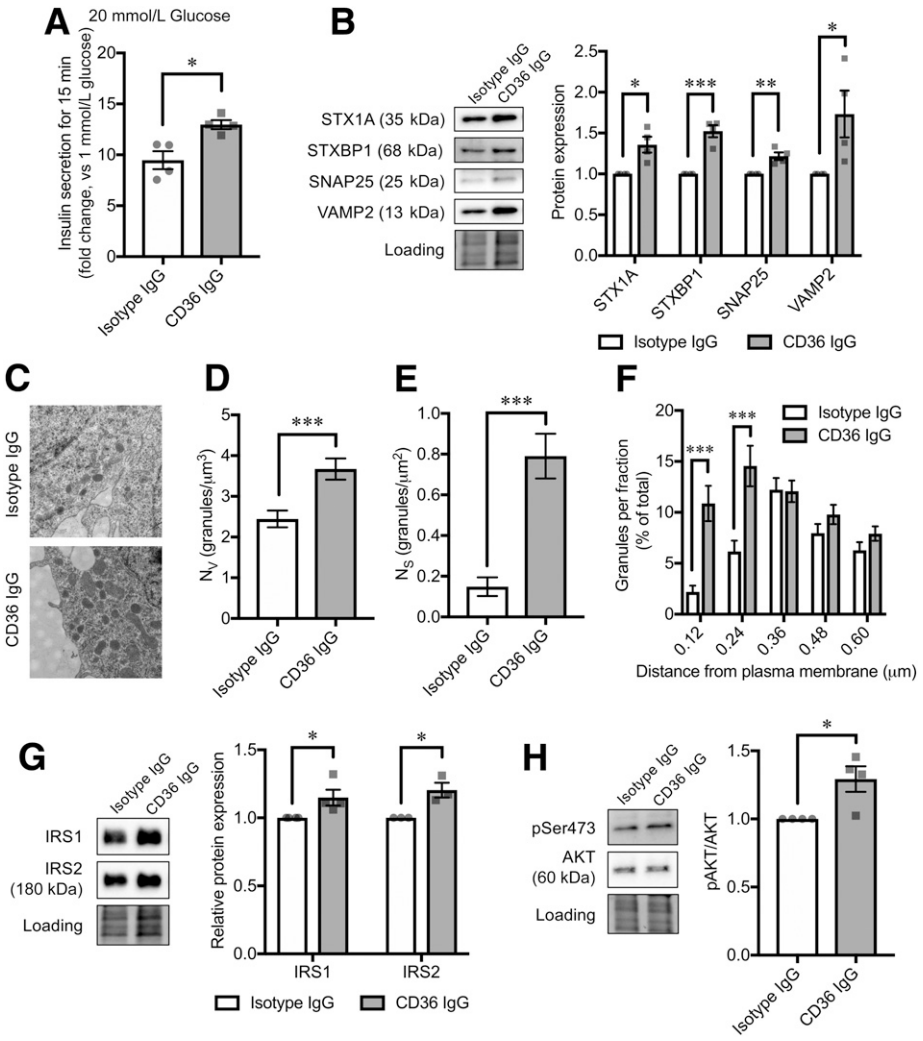

Figure 7— Effects of anti-CD36–neutralizing antibody on EndoC-βH1 cell functions. *A*: Insulin secretion at 20 mmol/L glucose for 15 min (fold change, 20 mmol/L glucose vs. 1 mmol/L glucose). $N = 4$ for each group. *B*: Exocytotic protein levels. Normalization factor (the total reference lane protein/total target lane protein) is the correction factor used to calculate the adjusted volume of target band. $N = 4$ for each group. *C–F*: Granule-distribution analyses on the electron micrographs of EndoC-βH1 cells. Original magnification ×43,000 (*C*). N_v (*D*) and N_s (*E*) were measured as volume density and surface density, respectively. The granules for which the center was located within 120 nm from the plasma membrane (a half-length of the mean granule diameter) were defined as docked. Relative distribution of granules at shown distance intervals from the center of granule to the plasma membrane is shown in *F*. The distance shown in the *x*-axis is the upper border of each fraction. $N =$ 20 cells for each group. *G*: IRS1 and IRS2 protein levels. $N = 4$ for each group. *H*: Phosphorylation levels of AKT Ser473 (pSer473). Phosphorylated protein signals were normalized to the total protein levels. $N = 4$ for each group. The total protein images obtained using the Stain-Free technology are shown as a loading control (Loading). The *P* values were determined by Student two-tailed *t* test (unpaired). $^*P < 0.05$; $^{**}P < 0.01$; $^{***}P < 0.001$.

CD36-mediated LCFA influx may induce intracellular ceramide accumulation by its de novo synthesis, which has been reported to cause AKT inactivation in β-cells (45). It has also been suggested that extracellular ceramide-induced AKT inactivation is dependent on a CD36-initiated inflammatory signaling cascade in β-cells (46). These previous findings support the model in which CD36 participates in exocytotic protein reduction through the suppression of the insulin-signaling PI3K/AKT pathway and its downstream transcription factors (Fig. 8).

Are our findings relevant for human T2D? We and others have earlier shown that reduced expression of exocytotic genes in islets occurs in T2D (17,19,47). In addition, restoration of exocytotic proteins in human β-cells could improve granule docking and exocytosis (19). These data are in line with possible in vivo effects of CD36 on first-phase insulin secretion, because it has been suggested that the reduced first-phase insulin secretion in T2D is due to the reduced pool of docked and primed insulin granules (48). Considering the overall roles of CD36 for insulin secretion as shown in the current study, obese individuals who have higher CD36 expression in β-cells may have a lower insulin secretion capacity due to exocytotic defects and consequently might be more prone to develop T2D. Such speculation could be

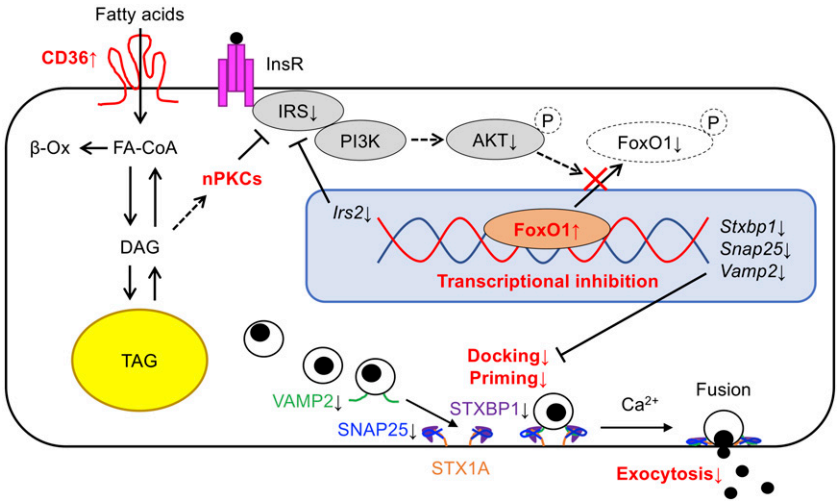

Figure 8—Model describing the possible involvement of CD36 in β-cell granule docking and exocytosis. CD36-mediated facilitation of lipid influx (including FAs) increases intracellular DAG, which leads to the translocation of nPKCs to the plasma membrane (activation of nPKCs). The activated nPKCs elicit abnormal phosphorylation of IRS1 and consequently attenuate PI3K/AKT signaling. The following retention of FoxO1 in the nucleus results in the transcriptional inhibition of Irs2 and exocytotic genes, which in turn impairs granule docking and priming with impaired exocytosis of insulin granules and reduced insulin secretion in β-cells as a consequence. β-Ox, β-oxidation; InsR, insulin receptor; TAG, triacylglycerol.

partly supported by the finding that CD36 expression in β-cells has been upregulated prior to the incidence of T2D, as there was no difference in *CD36* gene expression between IGT and T2D islets of obese donors in the RNA-seq study (Supplementary Fig. 7). In contrast, lower CD36 expression in β-cells might be advantageous to avoid T2D. The finding that obese donors with lower CD36 expression in islets seem to be protected against T2D encouraged us to test the therapeutic potential of CD36 functional blockade to improve β-cell function, especially exocytosis. The EndoC-βH1 cell line closely resembles human β-cells, especially in stimulus-secretion coupling (49). The cell line is also regarded as an appropriate screening platform for novel drug candidates for diabetes (50). We could detect CD36 protein in EndoC-βH1 cells, and the blockade of CD36 function on the cells led to increased exocytotic protein levels, improved granule docking, and enhanced first-phase insulin secretion. We believe the blockage of CD36 function could be an attractive approach to improve insulin secretion, especially in obesity-related T2D. A further study to test the CD36-neutralizing antibody on human islets of obese donors with T2D is warranted as the next step.

The importance of insulin signaling for β-cell function, especially in early phase insulin secretion, was previously demonstrated in β-cell–specific insulin receptor–deficient mice (51). However, a key molecule responsible for modulating β-cell insulin signaling in T2D has not been investigated previously. Intriguingly, the proposed mechanism to suppress β-cell insulin signaling by CD36 is considered similar to other insulin target organs (15,52), but the outcomes are unique to β-cells (i.e., defective exocytosis and reduced first-phase insulin secretion). CD36, therefore, may be a common denominator linking the two major etiologies of T2D (i.e., insulin resistance and defective insulin secretion). Taken together, our findings further highlight the pathogenic role of β-cell CD36 in the development of T2D, especially in relation to obesity.

Acknowledgments. The authors thank Anna-Maria Veljanovska Ramsay and Britt-Marie Nilsson (both from Lund University Diabetes Centre, Malmö, Sweden) as well as Momoyo Kawahara and Miyuki Takatori (both from Nippon Medical School, Tokyo, Japan) for technical assistance. The authors also thank Anneli Björklund (Karolinska Institute, Stockholm, Sweden) for providing the CD36-overexpressing INS-1 cell line and EXODIAB and the Nordic Network for Clinical Islet Transplantation for providing human islets and human islet data.

Funding. This study is financially supported by the Swedish Foundation for Strategic Research (IRC15-0067 to Lund University Diabetes Centre-Industrial Research Centre), Swedish Research Council (2009-1039 to EXODIAB; 349-2006-237 to Lund University Diabetes Centre; and project grants 2016-02124 and 2019-01406 to L.E.), Japan Society for the Promotion of Science (to M.N., J.L.S.E., and A.A.), European Foundation for the Study of Diabetes and Japan Diabetes Society (to M.N.), Insamlingsstiftelsen Diabetes Wellness Network Sverige (720-2964 JDWG to M.N.), Uehara Memorial Foundation (to M.N.), Scandinavia-Japan Sasakawa Foundation (to M.N.), Sumitomo Life Welfare Foundation (to M.N.), Nippon Medical School Alumni Association (to M.N.), Lotte Shigemitsu Prize (to A.A.), Albert Påhlsson Foundation (to J.L.S.E. and L.E.), Region Skåne-regional grant (ALF) (to L.E.), Novo Nordisk Foundation (to L.E.), and Swedish Diabetes Foundation (DIA2016-130 to L.E.).

Duality of Interest. No potential conflicts of interest relevant to this article were reported.

Author Contributions. L.E. supervised the project. M.N. and L.E. designed experiments, conducted data analysis, and wrote the manuscript. M.N., A.A., J.K.O., A.E., and A.W. performed experiments. J.L.S.E. analyzed RNA-seq data. H.S., C.B.W., and S.O. contributed with discussion and edited the manuscript. L.E. and M.N. are the guarantors of this work and, as such, had full access to all of the data in the study

and take responsibility for the integrity of the data and the accuracy of the data analysis.

References

1. Ling C, Groop L. Epigenetics: a molecular link between environmental factors and type 2 diabetes. Diabetes 2009;58:2718–2725
2. Franks PW, McCarthy MI. Exposing the exposures responsible for type 2 diabetes and obesity. Science 2016;354:69–73
3. Borén J, Taskinen MR, Olofsson SO, Levin M. Ectopic lipid storage and insulin resistance: a harmful relationship. J Intern Med 2013;274:25–40
4. Leibowitz G, Kaiser N, Cerasi E. β-cell failure in type 2 diabetes. J Diabetes Investig 2011;2:82–91
5. Unger RH. Lipotoxicity in the pathogenesis of obesity-dependent NIDDM. Genetic and clinical implications. Diabetes 1995;44:863–870
6. Rosengren AH, Braun M, Mahdi T, et al. Reduced insulin exocytosis in human pancreatic β-cells with gene variants linked to type 2 diabetes. Diabetes 2012;61:1726–1733
7. Poitout V, Robertson RP. Glucolipotoxicity: fuel excess and beta-cell dysfunction. Endocr Rev 2008;29:351–366
8. Oh YS, Bae GD, Baek DJ, Park EY, Jun HS. Fatty acid-induced lipotoxicity in pancreatic beta-cells during development of type 2 diabetes. Front Endocrinol (Lausanne) 2018;9:384
9. Hoppa MB, Collins S, Ramracheya R, et al. Chronic palmitate exposure inhibits insulin secretion by dissociation of Ca(2+) channels from secretory granules. Cell Metab 2009;10:455–465
10. Leibiger IB, Leibiger B, Berggren PO. Insulin signaling in the pancreatic beta-cell. Annu Rev Nutr 2008;28:233–251
11. Goldfine AB, Kulkarni RN. Modulation of β-cell function: a translational journey from the bench to the bedside. Diabetes Obes Metab 2012;14(Suppl. 3):152–160
12. Rhodes CJ, White MF, Leahy JL, Kahn SE. Direct autocrine action of insulin on β-cells: does it make physiological sense? Diabetes 2013;62:2157–2163
13. Kato T, Shimano H, Yamamoto T, et al. Granuphilin is activated by SREBP-1c and involved in impaired insulin secretion in diabetic mice. Cell Metab 2006;4:143–154
14. Noushmehr H, D'Amico E, Farilla L, et al. Fatty acid translocase (FAT/CD36) is localized on insulin-containing granules in human pancreatic beta-cells and mediates fatty acid effects on insulin secretion. Diabetes 2005;54:472–481
15. Wilson CG, Tran JL, Erion DM, Vera NB, Febbraio M, Weiss EJ. Hepatocyte-specific disruption of CD36 attenuates fatty liver and improves insulin sensitivity in HFD-fed mice. Endocrinology 2016;157:570–585
16. Ravassard P, Hazhouz Y, Pechberty S, et al. A genetically engineered human pancreatic β cell line exhibiting glucose-inducible insulin secretion. J Clin Invest 2011;121:3589–3597
17. Andersson SA, Olsson AH, Esguerra JL, et al. Reduced insulin secretion correlates with decreased expression of exocytotic genes in pancreatic islets from patients with type 2 diabetes. Mol Cell Endocrinol 2012;364:36–45
18. Fadista J, Vikman P, Laakso EO, et al. Global genomic and transcriptomic analysis of human pancreatic islets reveals novel genes influencing glucose metabolism. Proc Natl Acad Sci U S A 2014;111:13924–13929
19. Gandasi NR, Yin P, Omar-Hmeadi M, Ottosson Laakso E, Vikman P, Barg S. Glucose-dependent granule docking limits insulin secretion and is decreased in human type 2 diabetes. Cell Metab 2018;27:470–478.e4
20. Eich T, Ståhle M, Gustafsson B, et al. Calcium: a crucial potentiator for efficient enzyme digestion of the human pancreas. Cell Transplant 2018;27:1031–1038
21. Salunkhe VA, Ofori JK, Gandasi NR, et al. MiR-335 overexpression impairs insulin secretion through defective priming of insulin vesicles. Physiol Rep 2017;5:1–12
22. Vikman J, Ma X, Hockerman GH, Rorsman P, Eliasson L. Antibody inhibition of synaptosomal protein of 25 kDa (SNAP-25) and syntaxin 1 reduces rapid exocytosis in insulin-secreting cells. J Mol Endocrinol 2006;36:503–515
23. Hsieh YP, Ofori JA. Speciation of animal fat: needs and challenges. Crit Rev Food Sci Nutr 2017;57:1673–1680
24. Olofsson CS, Göpel SO, Barg S, et al. Fast insulin secretion reflects exocytosis of docked granules in mouse pancreatic B-cells. Pflugers Arch 2002;444:43–51
25. Wallin T, Ma Z, Ogata H, et al. Facilitation of fatty acid uptake by CD36 in insulin-producing cells reduces fatty-acid-induced insulin secretion and glucose regulation of fatty acid oxidation. Biochim Biophys Acta 2010;1801:191–197
26. Kaneko K, Ueki K, Takahashi N, et al. Class IA phosphatidylinositol 3-kinase in pancreatic β cells controls insulin secretion by multiple mechanisms. Cell Metab 2010;12:619–632
27. Cheng KK, Lam KS, Wu D, et al. APPL1 potentiates insulin secretion in pancreatic β cells by enhancing protein kinase Akt-dependent expression of SNARE proteins in mice. Proc Natl Acad Sci U S A 2012;109:8919–8924
28. Kitamura T. The role of FOXO1 in β-cell failure and type 2 diabetes mellitus. Nat Rev Endocrinol 2013;9:615–623
29. Haeusler RA, McGraw TE, Accili D. Biochemical and cellular properties of insulin receptor signalling. Nat Rev Mol Cell Biol 2018;19:31–44
30. Meur G, Qian Q, da Silva Xavier G, et al. Nucleo-cytosolic shuttling of FoxO1 directly regulates mouse Ins2 but not Ins1 gene expression in pancreatic beta cells (MIN6). J Biol Chem 2011;286:13647–13656
31. Copps KD, White MF. Regulation of insulin sensitivity by serine/threonine phosphorylation of insulin receptor substrate proteins IRS1 and IRS2. Diabetologia 2012;55:2565–2582
32. Zhang C, Klett EL, Coleman RA. Lipid signals and insulin resistance. Clin Lipidol 2013;8:659–667
33. Gao Z, Hwang D, Bataille F, et al. Serine phosphorylation of insulin receptor substrate 1 by inhibitor kappa B kinase complex. J Biol Chem 2002;277:48115–48121
34. De Fea K, Roth RA. Protein kinase C modulation of insulin receptor substrate-1 tyrosine phosphorylation requires serine 612. Biochemistry 1997;36:12939–12947
35. Schmitz-Peiffer C, Biden TJ. Protein kinase C function in muscle, liver, and beta-cells and its therapeutic implications for type 2 diabetes. Diabetes 2008;57:1774–1783
36. Schmitz-Peiffer C, Laybutt DR, Burchfield JG, et al. Inhibition of PKCepsilon improves glucose-stimulated insulin secretion and reduces insulin clearance. Cell Metab 2007;6:320–328
37. Hennige AM, Ranta F, Heinzelmann I, et al. Overexpression of kinase-negative protein kinase Cdelta in pancreatic beta-cells protects mice from diet-induced glucose intolerance and beta-cell dysfunction. Diabetes 2010;59:119–127
38. Pascual G, Avgustinova A, Mejetta S, et al. Targeting metastasis-initiating cells through the fatty acid receptor CD36. Nature 2017;541:41–45
39. Rorsman P, Renström E. Insulin granule dynamics in pancreatic beta cells. Diabetologia 2003;46:1029–1045
40. Martin C, Chevrot M, Poirier H, Passilly-Degrace P, Niot I, Besnard P. CD36 as a lipid sensor. Physiol Behav 2011;105:36–42
41. Carlsson C, Borg LA, Welsh N. Sodium palmitate induces partial mitochondrial uncoupling and reactive oxygen species in rat pancreatic islets in vitro. Endocrinology 1999;140:3422–3428
42. Laybutt DR, Preston AM, Akerfeldt MC, et al. Endoplasmic reticulum stress contributes to beta cell apoptosis in type 2 diabetes. Diabetologia 2007;50:752–763
43. Gao N, White P, Doliba N, Golson ML, Matschinsky FM, Kaestner KH. Foxa2 controls vesicle docking and insulin secretion in mature Beta cells. Cell Metab 2007;6:267–279
44. Aoyagi K, Ohara-Imaizumi M, Nishiwaki C, et al. Acute inhibition of PI3K-PDK1-Akt pathway potentiates insulin secretion through upregulation of newcomer granule fusions in pancreatic β-cells. PLoS One 2012;7:e47381
45. Chavez JA, Knotts TA, Wang LP, et al. A role for ceramide, but not diacylglycerol, in the antagonism of insulin signal transduction by saturated fatty acids. J Biol Chem 2003;278:10297–10303
46. Karunakaran U, Moon JS, Lee HW, Won KC. CD36 initiated signaling mediates ceramide-induced TXNIP expression in pancreatic beta-cells. Biochim Biophys Acta 2015;1852:2414–2422

47. Ostenson CG, Gaisano H, Sheu L, Tibell A, Bartfai T. Impaired gene and protein expression of exocytotic soluble N-ethylmaleimide attachment protein receptor complex proteins in pancreatic islets of type 2 diabetic patients. Diabetes 2006;55:435–440
48. Daniel S, Noda M, Straub SG, Sharp GW. Identification of the docked granule pool responsible for the first phase of glucose-stimulated insulin secretion. Diabetes 1999;48:1686–1690
49. Andersson LE, Valtat B, Bagge A, et al. Characterization of stimulus-secretion coupling in the human pancreatic EndoC-βH1 beta cell line. PLoS One 2015;10: e0120879
50. Tsonkova VG, Sand FW, Wolf XA, et al. The EndoC-βH1 cell line is a valid model of human beta cells and applicable for screenings to identify novel drug target candidates. Mol Metab 2018;8:144–157
51. Kulkarni RN, Brüning JC, Winnay JN, Postic C, Magnuson MA, Kahn CR. Tissue-specific knockout of the insulin receptor in pancreatic beta cells creates an insulin secretory defect similar to that in type 2 diabetes. Cell 1999;96:329–339
52. Ibrahimi A, Bonen A, Blinn WD, et al. Muscle-specific overexpression of FAT/CD36 enhances fatty acid oxidation by contracting muscle, reduces plasma triglycerides and fatty acids, and increases plasma glucose and insulin. J Biol Chem 1999;274:26761–26766